Reduced Carbon Solubility in Fe Nanoclusters and Implications for the Growth of Single-Walled Carbon Nanotubes

A. R. Harutyunyan,[1,*,†] N. Awasthi,[2] A. Jiang,[2] W. Setyawan,[2] E. Mora,[1] T. Tokune,[1] K. Bolton,[3] and S. Curtarolo[2,*,‡]

[1]*Honda Research Institute USA, Inc., 1381 Kinnear Road, Columbus, Ohio 43212, USA*

[2]*Department of Mechanical Engineering and Materials Science, Duke University, Durham, North Carolina 27708, USA*

[3]*University College of Borås, SE-501 90 Borås and Physics Department, Göteborg University, SE-412 96 Göteborg, Sweden*

(Received 26 October 2007; published 14 May 2008)

Fe nanoclusters are becoming the standard catalysts for growing single-walled carbon nanotubes via chemical vapor decomposition. Contrary to the Gibbs-Thompson model, we find that the reduction of the catalyst size requires an increase of the minimum temperature necessary for the growth. We address this phenomenon in terms of solubility of C in Fe nanoclusters and, by using first-principles calculations, we devise a simple model to predict the behavior of the phases competing for stability in Fe-C nanoclusters at low temperature. We show that, as a function of particle size, there are three scenarios compatible with steady state growth, limited growth, and no growth of single-walled carbon nanotubes, corresponding to unaffected, reduced, and no solubility of C in the particles.

DOI: 10.1103/PhysRevLett.100.195502 PACS numbers: 61.46.Df, 64.70.D−, 65.80.+n, 82.60.Qr

Among the established methods for single-walled carbon nanotubes (SWCNTs) synthesis, the low-temperature catalytic chemical vapor decomposition (CCVD) technique is more appropriate for growing nanotubes on a substrate at a target position [1–5]. Considering the vapor-liquid-solid model as the most probable mechanism for SWCNT growth [6–8], an approach for lowering the growth temperature is the reduction of the catalyst size. In fact, the Gibbs-Thompson model predicts a decrease of the melting temperature with decreasing cluster size [9–11], and the synthesis temperature has been shown to be correlated with the catalyst-carbon melting and eutectic points [12–14]. While small catalyst particles nucleate small diameter tubes, they also affect the morphology of the formed carbon structures [15], the kinetics of the growth [16,17], and the solubility of carbon available for the growth process. The latter requires the understanding of the effect of the thermodynamic state on the catalytic activity of the particle, which is an important yet open question since the lack of a rational description of binary phase diagrams at the nanoscale. In this work, we address such problems by studying the solubility of C in Fe nanoclusters, with size-dependent CCVD growth of SWCNTs and with *ab initio* modeling of the stability of the competing phases.

In our experiments, Fe catalysts supported on alumina powder were prepared using the common impregnation method [7]. To find the minimum synthesis temperature, $T^{\min}_{\text{synth}}$, as a function of catalyst size, different particles' dimensions were obtained by varying the Fe:Al_2O_3 molar ratio 1:15, 1:25, 1:50, and 1:100, [18] corresponding to particles of diameters $\sim 3 \pm 0.6$, $\sim 2 \pm 0.8$, $\sim 1.4 \pm 0.7$, and $\sim 1.3 \pm 0.7$ nm, respectively. The growth of SWCNTs was performed with CCVD at temperatures between 650 °C–900 °C for 90 min over the prereduced catalysts [19]. To avoid increasing the catalyst temperature, methane was used as the carbon source since the formation of SWCNTs from methane is not exothermic. For each case $T^{\min}_{\text{synth}}$ was determined by analyzing the Raman spectra (Thermo Nicolet Almega Raman spectrometer equipped with a CCD detector, laser excitations of 532 and 785 nm).

Figure 1 shows the $T^{\min}_{\text{synth}}$ dependence on the Fe:Al_2O_3 molar ratio. The inset presents a typical example of Raman spectra after the synthesis between 820 °C and 865 °C. As can be seen from the molar ratio of 1:50, SWCNTs can be grown at 865 °C but not at 850 °C even though carbon deposition is observed. In this case, $T^{\min}_{\text{synth}}$ was estimated to be $\sim 865 \pm 9$ °C. We find that $T^{\min}_{\text{synth}}$ increases with de-

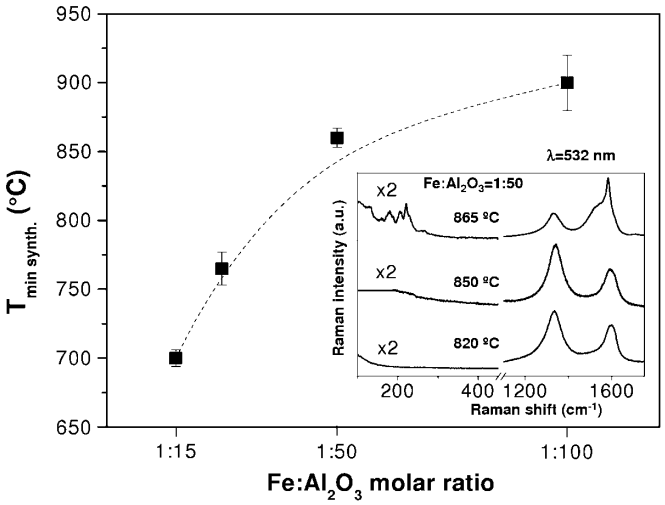

FIG. 1. Evolution of minimum synthesis temperature ($T^{\min}_{\text{synth}}$) for growing SWCNTs with Fe:Al_2O_3 molar ratio. The inset shows the Raman spectra for minimum synthesis temperature versus Fe:Al_2O_3 molar ratio. The inset shows the Raman spectra for samples obtained with a catalyst molar ratio of 1:50.

creasing catalyst size (molar ratio), contrary to what may be expected from the Gibbs-Thompson model [10]. This observation indicates that decomposition of the hydrocarbon alone is not enough to grow nanotubes and that the temperature must be increased to ensure that a certain amount of carbon dissolves into the particle (considering that the maximum solubility of C in Fe depends on the catalyst size, as shown later). In fact, temperature must be increased to overcome the loss of solubility of C in the catalytically active phase competing for thermodynamical stability with a nucleating carbide, and not only to enhance diffusion of C (otherwise below $T^{\min}_{\text{synth}}$ we would have shorter nanotubes instead of their absence).

We believe that the origin of this apparent paradox lies in a novel phenomenon, i.e., a reduced solubility of C in Fe nanoparticles. Within the vapor-liquid-solid framework with bulk diffusion as the rate-limiting step [7,20–22], this implies an increase of temperature to achieve a comparable amount of dissolved carbon to allow growth. In Ref. [10] we have shown that the eutectic point (x^C_{eut}, T_{eut}) of Fe-C clusters shifts toward lower carbon concentrations, x^C_{eut}, with decreasing particle size (Fig. 8 of [10]). Because of the high energetic cost for bringing bulk cementite off stoichiometry [in the Fe-C phase diagrams Fe_3C forms two-phase regions with austenite (γ) and ferrite (α) without going off stoichiometry [23]], the most probable cause of the shift of x^C_{eut} is a reduced solubility of C.

The accurate analysis of the phenomenon can be achieved by calculating the interplay between the phases competing for stability at the temperatures of the process. For nanoparticles, this task is generally unsolvable, although qualitative information can be extracted from approximate zero-temperature first-principles modeling. In such approaches, by comparing the formation energies of the candidate phases, we determine the stability of the system at low T and give indications for higher temperature behavior. The *ab initio* simulations presented here are performed with VASP [24], using projector augmented waves [25] and exchange-correlation functionals as parametrized by Perdew, Burke, and Ernzerhof [26] for the generalized gradient approximation. Simulations are carried out with spin polarization, at zero temperature, and without zero-point motion. All structures are fully relaxed. Numerical convergence to within about 2 meV/atom is ensured by enforcing a high energy cutoff (500 eV) and dense **k** meshes.

Our model is based on the following assumptions: (i) *Mechanism.* The behavior of carbon is determined by the interplay of four competing phases as a function of catalyst size: pure bcc Fe, C dissolved in ferrite (α-FeC_x), ordered cementite (Fe_3C), and carbon SWNTs [7,23]. The pure-Fe phase is taken to be bcc because our simulations are aimed to explore the low-temperature regime of catalytic growth. The α-FeC_x phase is simulated by taking samples of bcc supercells with different concentrations of interstitial carbon ($Fe_{32}C$, $Fe_{24}C$, $Fe_{16}C$). We are not required to generate truly random phases by using the special quasirandom structure formalism because the low concentration of carbon guarantees enough distance between replica of C to achieve convergence. In addition, higher concentrations of C are not required to be explored because even in bulk α-FeC_x the solubility is small [23]. (ii) *Carbon source.* Free carbon atoms come from the dissociation of the feedstock on the surface of pure-Fe and random FeC_x catalysts only. Formation of cementite stops the process due to its different activity and diffusion properties (as show in Fig. 1 of [7] and references therein). (iii) *Nanotube diameter.* To minimize the curvature energy of the tube, active catalysts produce nanotubes that have a similar diameter as the particle (CVD experiments have shown a clear correlation between the two diameters [27]). (iv) *Size-pressure approximation.* In nanoparticles, surface curvature and superficial dangling bonds are responsible for internal stress fields which modify the atomic bond lengths inside the particles. The phenomenon can be modeled with the Young-Laplace equation $\Delta P = 2\gamma/R$ where the proportionality constant γ (surface tension for liquid particles) can be calculated with *ab initio* methods. As a first approximation, by neglecting all the surface effects not included in the curvature, the study of phase diagrams for spherical particles can be mapped onto the study of phase diagrams for bulk systems under the same pressure produced by the curvature, as depicted in Fig. 2 [28]. It is

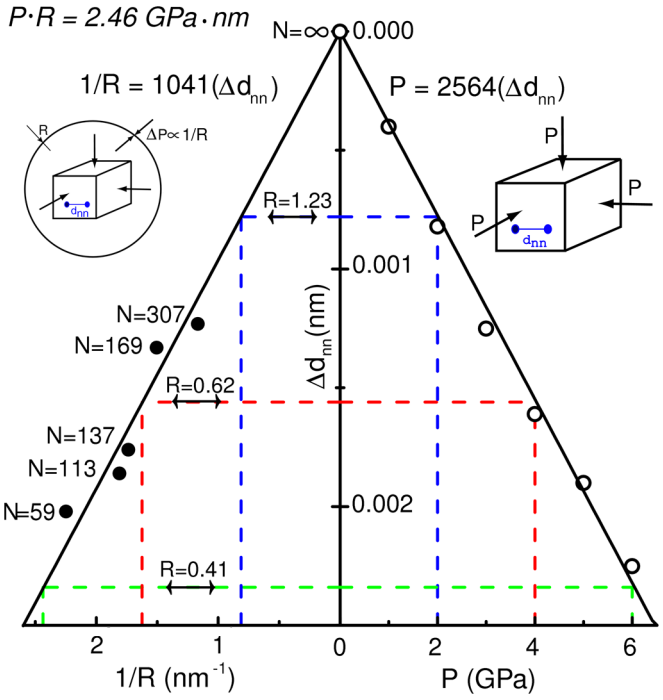

FIG. 2 (color online). Size-pressure approximation for Fe nanoparticles. Given a spherical particle, we estimate the hydrostatic pressure due to the surface curvature by calculating the deviation of the average bond length inside the cluster, $\Delta d_{nn} \equiv d^0_{nn} - d_{nn}$, and comparing it to the deviation of the bond length for the bulk material as a function of hydrostatic pressure.

worth mentioning that our reference for carbon is taken to be the zero pressure nanotube phase, different from the other carbon references used for investigating Fe-C under pressure [29–31].

Figure 2 shows the implementation of the ''size-pressure approximation'' for Fe nanoparticles. On the left-hand side we show the *ab initio* calculations of the deviation of the average bond length inside the cluster $\Delta d_{nn} \equiv d_{nn}^0 - d_{nn}$ ($d_{nn}^0 = 0.2455$ nm is our bulk bond length), for bcc particles of size $N = 59$, 113, 137, 169, 307, and ∞ (bulk) as a function of the inverse radius ($1/R$). The particles were created by intersecting a bcc lattice with different size spheres. The particle radius is defined as $1/R \equiv 1/N_{\mathrm{scp}} \sum_i 1/R_i$ where the sum is taken over the atoms belonging to the surface convex polytope (N_{scp} vertices) and R_i are the distances to the geometric center of the cluster [32]. The left straight line is a linear interpolation between $1/R$ and Δd_{nn} calculated with the constraint of passing through $1/R = 0$ and $\Delta d_{nn} = 0$ ($N = \infty$, bulk). The right-hand side shows the *ab initio* value of d_{nn} in bulk bcc Fe as a function of hydrostatic pressure P. The straight line is a linear interpolation between P and Δd_{nn} calculated with the constraint of passing through $P = 0$ and $\Delta d_{nn} = 0$ (bulk lattice). By following the colored dashed paths indicated by the arrows we can map the analysis of nanoparticles' stability as function of R onto bulk stability as function of P, and obtain the relation between the radius of a particle or nanotube and the effective pressure $P \cdot R = 2.46$ GPa $\cdot$ nm. It is important to mention that our $\gamma = 1.23$ J/m^2 is not a real surface tension but an *ab initio* fitting parameter describing size-induced stress in nanoparticles. In addition, it compares well with the experimental value of the surface tension of bulk Fe at its melting point $\sim$1.85 J/m^2 [33].

Figure 3 shows the evolution of competing phases as a function of concentration and particle's size. In Figs. 3(a)–3(d), we plot formation energies, $E_f[\mathrm{Fe}_{1-y}\mathrm{C}_y] \equiv E[\mathrm{Fe}_{1-y}\mathrm{C}_y] - (1-y)E[\mathrm{Fe}] - yE[\mathrm{C}]$, calculated with respect to the pure constituents of the reaction, bcc Fe and carbon SWCNTs (with the same diameter as the particle). The dashed gray (green) lines interpolating $\mathrm{Fe_{16}C}$ through Fe are used to estimate the formation energies of the random phase with maximum solubility of carbon (α-$\mathrm{FeC}^{\mathrm{sol}}_{\sim 0.001\,02}$, black squares near the origin in Fig. 3 labeled as $\mathrm{FeC}_x^{\star}$) corresponding to 0.022 wt % [23]. A structure at a given composition is considered stable (at zero temperature and without zero-point motion) if it has the lowest formation energy for any structure at this composition and, if on the binary phase diagram, it lies below the *convex hull of tie lines* connecting all the other stable structures [34,35]. Phases lying above the convex hull and with small positive formation energies might be explored by the thermodynamics of the system through configurational and vibrational entropic promotion.

By varying the radius of the particle, the stability of the competing phases, α-FeC_x and $\mathrm{Fe_3C}$, changes considerably. There are three possible scenarios. *Scenario I* is shown in 3(a) and 3(b). For big particles, $R \gg R_{\mathrm{min}}$, $\mathrm{Fe_3C}$ has formation energy higher than the maximum solubility phase (α-$\mathrm{FeC}^{\mathrm{sol}}_{\sim 0.001\,02}$). Therefore the pollution of carbon at low and medium temperature cannot cause the big particle to undergo phase transition by nucleating cementite. Hence, such particles remain in the catalytically active random $\alpha\mathrm{FeC}_x$ state, by keeping their concentration of carbon between 0% and $\sim$0.102% [10] (solubility is unaffected), and by implying a balance between in and out flows of carbon which can guarantee the steady state growth of nanotubes. Thermodynamically, in this regime, SWCNTs, multiwalled carbon nanotubes, and carbon fibers could be grown indefinitely and the only limitation is the availability of carbon feedstock [36]. Thus, experiments performed with particles of these sizes would be described by Arrhenius equations governing catalytic activity and diffusion properties. The minimum radius R_{min} can be estimated by interpolating the pressure at which the energy of $\mathrm{Fe_3C}$ and α-$\mathrm{FeC}^{\mathrm{sol}}_{\sim 0.001\,02}$ are equal, and by mapping such pressure in the size-pressure relation of Fig. 2. We obtain $P \sim 4.3$ GPa and $R_{\mathrm{min}} \sim 0.58$ nm. *Scenario II* is shown in 3(c). For particles of size $R \sim R_{\mathrm{min}}$, the maxi-

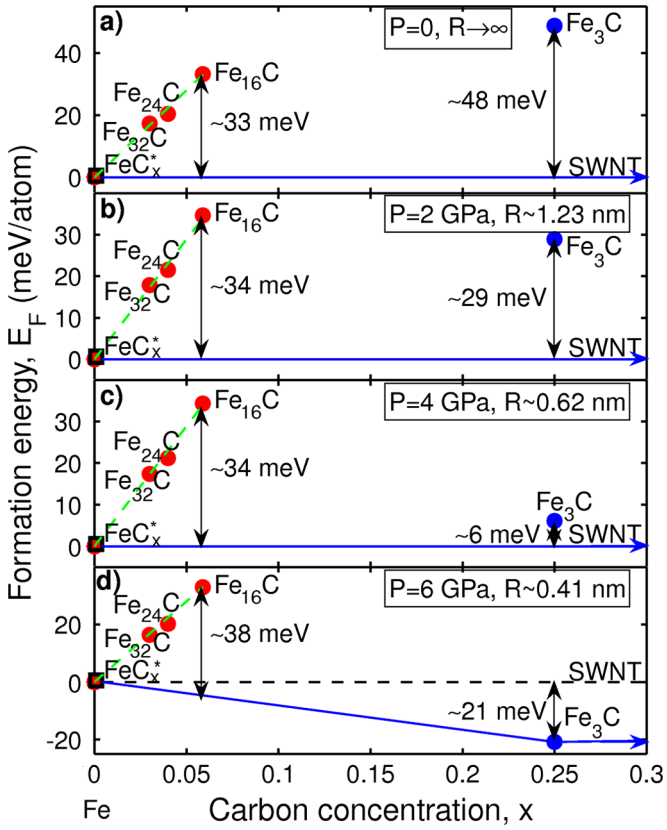

FIG. 3 (color online). The scenarios described in the text with their implication in CVD SWCNT growth with Fe nanocatalysts. P is the pressure at which the calculations are performed and R is the radius of the corresponding SWCNT within the size-pressure approximation. $E_f[\mathrm{Fe_3C}] = E_f[\alpha\text{-}\mathrm{FeC}^{\mathrm{sol}}_{\sim 0.001\,02}]$ for $R_{\mathrm{min}} \sim 0.58$ nm ($P \sim 4.3$ GPa).

mum solubility phase and Fe_3C have similar formation energies. The energetically competing Fe_3C causes depletion of C in α-Fe C (reduced solubility), nucleation of ordered Fe_3C, and overall reduction of catalytically active random Fe. If exposed to hydrocarbons at elevated temperatures, such particles would be capable of dissociating carbon and growing SWCNTs with concomitant nucleation of cementite. Such nucleation slowly poisons the particle and terminates the growth. In this regime, SWCNTs can be produced up to a certain critical length depending on the net flow of carbon. By varying R, the critical length goes from infinity ($R > R_{\min}$) to zero ($R < R_{\min}$). Experiments performed with particles of size $R \sim R_{\min}$ would show on and off growth at low temperature and Arrhenius behavior at high temperature. *Scenario III* is shown in 3(d). By further reducing the size of the particle, $R \ll R_{\min}$, the formation energy of cementite becomes negative ($E_f[\alpha\text{-}FeC^{\text{sol}}_{\sim 0.001\,02}]$ is always very close to zero). The stability of Fe_3C over the range 0%–25% carbon in the phase diagram indicates that the nucleation of Fe_3C occurs simultaneously with the carbon pollution. The particle transforms into Fe_3C as rapidly as the availability of feedstock allows; thus, no random phase coexists at low temperature (maximum solubility of C is zero), and no outflow of carbon occurs. Particles with $R < R_{\min}$ cannot grow SWCNTs, and $R_{\min}$ can be considered as a lower limit for SWCNTs' size in low-temperature CVD growth with Fe nanocatalysts. Experiments performed with such particles would result in Fe_3C nanoparticles and no appreciable nanotube productions.

We address the extension of the model to higher temperatures in a qualitative framework [37]. Increasing the temperature of the reaction and considering fcc Fe nanoparticles has two consequences. Fe_3C becomes stable at medium temperature [23] and, by reducing particle size, the stability versus size follows similar arguments as the case of the bcc reference. Thus $R_{\min} \rightarrow \infty$ and a steady state SWCNT growth is, *a priori*, unobtainable. However, since the maximum solubility of C in austenite γ-FeC_x is bigger than in ferrite α-FeC_x [due to the fact that interstitial holes in the fcc lattice are larger than those in the bcc lattices (~ 2.0 wt % in γ-FeC_x [23])], the life of the catalytic particle can somehow be longer than the previous scenarios II and III, and the grown SWCNTs can be quite long. The lack of steady state at high temperature can be addressed by alloying the nanoparticle with other metals to reduce cementite stability and by simultaneously promoting other more stable alloyed random phases with considerable catalytic activity. Even for Ni catalysts, C solubility has been suggested to be a key quantity to control nucleation of nanotubes [38].

We acknowledge helpful discussions with A. Kolmogorov, H. Baranger, T. Tan, N. Li, A. Ferrari, S. Hofmann, F. Cervantes-Sodi, and G. Csany. The authors are grateful for computer time allocated at the Swedish National Supercomputing and at the Teragrid facilities. This research was supported by Honda Research Institute USA, Inc. S. C. is supported by ONR (N00014-07-1-0878) and NSF (DMR-0639822).

*Corresponding author.
†aharutyunyan@oh.hra.com
‡stefano@duke.edu

[1] C. Journet *et al.*, Nature (London) **388**, 756 (1997).
[2] A. Thess *et al.*, Science **273**, 483 (1996).
[3] M. Cantoro *et al.*, Nano Lett. **6**, 1107 (2006).
[4] S. Maruyama *et al.*, Chem. Phys. Lett. **360**, 229 (2002).
[5] C. Klinke *et al.*, Phys. Rev. B **71**, 035403 (2005).
[6] A. Gorbunov *et al.*, Carbon **40**, 113 (2002).
[7] A. R. Harutyunyan *et al.*, Appl. Phys. Lett. **90**, 163120 (2007).
[8] H. Kanzow and A. Ding, Phys. Rev. B **60**, 11 180 (1999).
[9] A. A. Chernov, *Modern Crystallography* (Springer, Berlin, 1984), Vol. 3.
[10] A. Jiang *et al.*, Phys. Rev. B **75**, 205426 (2007).
[11] F. Ding *et al.*, Appl. Phys. Lett. **88**, 133110 (2006).
[12] Y. Saito, Carbon **33**, 979 (1995).
[13] L. Alvarez *et al.*, Chem. Phys. Lett. **342**, 7 (2001).
[14] A. R. Harutyunyan *et al.*, Appl. Phys. Lett. **87**, 051919 (2005).
[15] Y. Li *et al.*, Chem. Mater. **13**, 1008 (2001).
[16] S. Helveg *et al.*, Nature (London) **427**, 426 (2004).
[17] S. Hofmann *et al.*, Nano Lett. **7**, 602 (2007).
[18] A. R. Harutyunyan *et al.*, J. Appl. Phys. **100**, 044321 (2006).
[19] A. R. Harutyunyan *et al.*, Nano Lett. **2**, 525 (2002).
[20] R. S. Wagner *et al.*, Appl. Phys. Lett. **4**, 89 (1964).
[21] R. T. K. Baker *et al.*, J. Catal. **26**, 51 (1972).
[22] R. T. K. Baker *et al.*, Carbon **13**, 17 (1975).
[23] P. Villars *et al.*, *Pauling File* (ASM International, Metals Park, OH, 2003).
[24] G. Kresse and J. Hafner, Phys. Rev. B **47**, 558 (1993).
[25] P. E. Blochl, Phys. Rev. B **50**, 17 953 (1994).
[26] J. P. Perdew, K. Burke, and M. Ernzerhof, Phys. Rev. Lett. **77**, 3865 (1996).
[27] A. G. Nasibulin *et al.*, Carbon **43**, 2251 (2005), and references therein.
[28] Since the amount of C present in the Fe particle is limited, we take γ to be independent of the C concentration.
[29] Y. Yang and L. Deng, in *Proceedings of the 38th Lunar and Planetary Conference, Houston, TX, 2007* (Lunar and Planetary Institute, Houston, 2007), p. 1231.
[30] B. J. Wood, Earth Planet. Sci. Lett. **117**, 593 (1993).
[31] A. A. Zhukov, Metal Sci. Heat Treat. **30**, 249 (1988).
[32] The radius is so defined because "$1/R_i$" are the factors producing internal stress the particle.
[33] H. S. Kim *et al.*, J. Mater. Res. **21**, 1399 (2006).
[34] S. Curtarolo *et al.*, Phys. Rev. Lett. **91**, 135503 (2003).
[35] S. Curtarolo *et al.*, CALPHAD: Comput. Coupling Phase Diagrams Thermochem. **29**, 163 (2005).
[36] R. F. Wood *et al.*, Phys. Rev. B **75**, 235446 (2007).
[37] J.-F. Lin *et al.*, Phys. Rev. B **70**, 212405 (2004).
[38] H. Amara *et al.*, Phys. Rev. Lett. **100**, 056105 (2008).